Photoassociation and optical Feshbach resonances in an atomic Bose-Einstein condensate: Treatment of correlation effects

Pascal Naidon* and Françoise Masnou-Seeuws
Laboratoire Aimé Cotton, CNRS, Bâtiment 505 Campus d'Orsay, 91405 Orsay Cedex, France
(Received 17 October 2005; revised manuscript received 31 January 2006; published 18 April 2006)

In this paper we formulate the time-dependent many-body theory of photoassociation in an atomic Bose-Einstein condensate with realistic interatomic interactions, using and comparing two approximations: the *first-order cumulant* approximation [Phys. Rev. A **65**, 033601 (2002)], and the *reduced pair wave* approximation [Phys. Rev. A **68**, 033612 (2003)]. The two approximations differ only by the way a pair of condensate atoms is influenced by the mean field at short interatomic separations. In both cases we identify two different regimes of photoassociation: the *adiabatic* regime and the *coherent* regime. The threshold for the so-called "rogue dissociation" [Phys. Rev. Lett. **88**, 090403 (2002)] (where the Gross-Pitaevskiĭ model breaks down) is found to be different in each regime, shedding new light on the experiment of McKenzie *et al.* [Phys. Rev. Lett. **88**, 120403 (2002)]. Comparing numerical solutions for the two approximations with the Gross-Pitaevskiĭ predictions, we find two different effects: reduction of the photoassociation rate at short times, and creation of correlated pairs of atoms when the laser intensity is switched on rapidly. We also observe effects on the symmetry of the photoassociation line shapes, giving the possibility to experimentally distinguish between the two approximations.

DOI: 10.1103/PhysRevA.73.043611 PACS number(s): 03.75.Nt, 03.75.Kk, 34.50.−s

I. INTRODUCTION

The possibility to create molecular condensates opens new research avenues. These include test of fundamental symmetries [1,2], determination of fundamental constants through molecular spectroscopy with unprecedented accuracy, creation of molecular lasers and invention of a coherent super chemistry [3] at ultralow temperatures. Since direct laser cooling or sympathetic cooling appear more difficult for molecules than for atoms, many experimental groups have worked on procedures to transform an atomic quantum degenerate gas into a molecular condensate. Over the last two years a wealth of new experimental results have appeared about formation of molecules in a degenerate gas, starting either from an atomic Bose-Einstein condensate [4–8] or from an atomic Fermi gas [9–15].

So far the most successful scheme to produce molecules in a condensate involves an adiabatic sweep near a Feshbach resonance by varying in time the strength of an external magnetic field. However, the resulting Feshbach molecules are usually in a highly-excited vibrational level of the ground state interatomic potential and decay rapidly due to collisional quenching. An alternative would consist in varying the frequency of a laser in a photoassociation experiment, thereby sweeping across an optically induced Feshbach resonance. Such resonances have already been discussed in theoretical papers [16–18] and explored in recent experiments [19–21]. These resonances are in many ways similar to the magnetic Feshbach resonances, except that the resonant state is an electronically excited state with a usually very short lifetime due to spontaneous emission. As we shall see in this paper, this qualitatively changes the many-body properties of the system. On the other hand, photoassociation offers more experimental possibilities by varying in time the frequency or/and the intensity of the laser [22]. In particular, the use of shaped laser pulses opens the way to better control in this domain. For instance, by using a series of shaped pulses it should be possible to quickly transfer vibrationally excited molecules created via a magnetic Feshbach resonance to their ground vibrational state [23]. Photoassociation with pulsed lasers could therefore solve the problem of the short lifetime of molecular condensates, in particular bosonic dimers.

Mixed atomic and molecular condensates, formed by magnetic or optically induced Feshbach resonances, are typically described in the mean-field approximation, corresponding to two coupled Gross-Pitaevskiĭ equations [3,24,25]. This may not be sufficient when correlations play a significant role. For instance, they must be introduced in the theoretical models [26–30] to reproduce the damping in the observed [4] oscillations between the atomic and the molecular components of a condensate exposed to a time-dependent magnetic field.

In the case of an isolated resonance, it may be sufficient to describe the microscopic quantum dynamics with effective interactions such as contact or separable potentials, involving parameters fitted on two-body calculations. However, in the more general case of photoassociation with shaped laser pulses, many levels may be involved; several theoretical studies [31–33] investigating photoassociation with chirped pulses at a two-body level have shown a great sensitivity to the details of the molecular potentials.

A general treatment of photoassociation in a Bose-Einstein condensate should therefore be able to take both correlations and realistic interactions into account. To achieve this goal, we will consider two methods:

*Electronic address: pascal@nist.gov

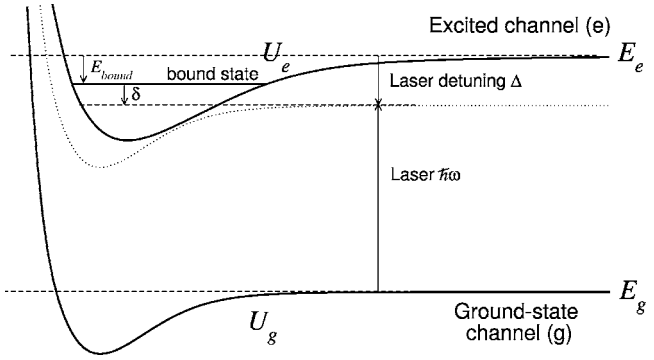

FIG. 1. Scheme of the photoassociation process.

(i) In a series of papers, [29,34–36] the Oxford group has developed a method based on a truncation of the expansion of correlation functions in terms of noncommutative cumulants [37]. The method to first order, hereafter referred to as *first-order cumulant approximation*, has been used so far assuming a separable interatomic potential, which was sufficient to successfully interpret magnetic Feshbach experiments [4,35].

(ii) In a previous paper [38], hereafter referred to as paper I, we have revisited the treatment of photoassociation and Feshbach resonances following another approach, hereafter referred to as the *effective pair wave approach*. This work generalizes the ideas of Cherny and Shanenko [39,40] to two coupled channels.

The present paper goes further by numerically solving the effective pair wave equations as well as the cumulant equations with realistic potentials. It is organized as follows: In Sec. II we recall the usual two-channel description of photoassociation for a pair of atoms. In Sect. III we give the coupled equations for a two-channel description of photoassociation in a condensate, using either the *first-order cumulant*, or *reduced pair wave* approximations. In Sec. IV we make a connection between these equations and the usual mean-field approximation of Ref. [25] for an isolated resonance. This enables us to determine the different regimes and conditions for which correlations play an important role. Section V describes the numerical methods used to solve the coupled equations given in Sec. II. In Sec. VI we present and discuss the results of our numerical calculations for high-intensity photoassociation in a sodium condensate, starting from the experimental conditions of Ref. [41]. We conclude in the appendix. In this paper we give scattering lengths in units of the Bohr radius $a_0=0.529177\times10^{-10}$ m.

II. TWO-BODY THEORY FOR PHOTOASSOCIATION

Let us first recall to the standard two-channel model describing the photoassociation reaction for two atoms [42,43], schematized in Fig. 1. In the ground (open) channel, the two atoms interact through a potential $U_g(r)$, r being the internuclear separation. A time-dependent radiative coupling can excite them to a second (closed) channel where they interact through a potential $U_e(r)$. We assume that $U_e(\infty)\to0$, $U_g(\infty)\to0$, and call E_g, E_e the dissociation limit energies of the atoms in the ground and excited channels respectively. We choose to set the origin of energies to $E_g=0$. The relative motion of the atoms is described by a two-component wave function ϕ, one component for each channel. At low temperature, only s-wave scattering is relevant, and we shall neglect rotation effects so that only the radial parts $\phi_g(r,t)$, $\phi_e(r,t)$ of these components are considered.

The radiative coupling is due to a laser red detuned by $\hbar\Delta$ relative to an atomic resonance line. In a classical picture, its electric field oscillates as $\cos(\omega t)$ at a pulsation $\omega=(E_e-E_g-\Delta)/\hbar$, and couples with the transition dipole moment $\mathbf{D}(r)$ of the two atoms between the two electronic states. Using the rotating wave approximation [44], it is possible to eliminate the rapid oscillations in the coupling term by defining new wave functions

$$\tilde{\phi}_e(r,t)=e^{i\omega t}\phi_e(r,t) \tag{1}$$

so that the the time-dependent Schrödinger equation becomes [32]

$$i\hbar\frac{\partial}{\partial t}\begin{pmatrix}\phi_g(r,t)\\ \tilde{\phi}_e(r,t)\end{pmatrix}=\mathbf{H}^{(2)}(r,t)\begin{pmatrix}\phi_g(r,t)\\ \tilde{\phi}_e(r,t)\end{pmatrix}, \tag{2}$$

where we have introduced the effective two-channel Hamiltonian

$$\mathbf{H}^{(2)}(r,t)=\begin{pmatrix}\hat{\mathbf{T}}+U_g(r) & W(t)\\ W(t) & \hat{\mathbf{T}}+U_e(r)+\Delta\end{pmatrix}. \tag{3}$$

It contains the relative kinetic energy operator $\hat{\mathbf{T}}=-\frac{\hbar^2\nabla^2}{m}$ and a coupling term

$$W(r,t)\approx W(t)=-\frac{1}{2}\sqrt{\frac{2I(t)}{c\epsilon_0}}D, \tag{4}$$

where $I(t)$ is the intensity of the laser, the constants c and ε_0 are, respectively, the light velocity and the vacuum permittivity, and D is one component of the dipole moment operator, depending upon the polarization of the laser, and assumed to be r indedependent.

III. PHOTOASSOCIATION THEORY FOR A CONDENSATE

A. General description

A Bose-condensed system is usually described in terms of a macroscopic one-body wave function Ψ and a residual noncondensate one-body density matrix R'. The evolution of these quantities depend on higher-order density matrices, which can be written in terms of pair, triplet, etc., wave functions (see Appendix and Ref. [38]). In particular, the condensate wave function Ψ is coupled to a macroscopic pair wave function Φ describing the motion of two condensate atoms.

Considering now photoassociation in a condensate, we introduce a two-component macroscopic pair wave function Φ: the usual component Φ_g in the ground (open) channel, and a new component Φ_e in the excited (closed) channel. The component in the open channel is connected at large

distances to a product of condensate wave functions Ψ, whereas the component in the closed channel corresponds to a bound vibrational level and vanishes at large distances

$$\Phi(\mathbf{x},\mathbf{y},t)=\begin{pmatrix}\Phi_g(\mathbf{x},\mathbf{y},t)\\ \Phi_e(\mathbf{x},\mathbf{y},t)\end{pmatrix}\xrightarrow[|\mathbf{x}-\mathbf{y}|\to\infty]{}\begin{pmatrix}\Psi(\mathbf{x},t)\Psi(\mathbf{y},t)\\ 0\end{pmatrix}.$$

For simplicity, we will consider a homogeneous system. In this case, the condensate wave function $\Psi(\mathbf{x},t)$ is uniform, and the functions $\Phi(\mathbf{x},\mathbf{y},t)$ and $R'(\mathbf{x},\mathbf{y},t)$ depend only on the relative coordinate $\mathbf{x}-\mathbf{y}=\mathbf{r}$. Assuming an isotropic situation with s-wave scattering only we shall simply write $\Psi(t)$, $\Phi_g(r,t)$, $\Phi_e(r,t)$, and $R'(r,t)$ for the condensate wave function, the two components of the pair wave function, and the density matrix for the noncondensate atoms in the ground state.

B. Theory with contact interactions

In many theoretical treatments of the condensed Bose gas [45,46], binary interactions between atoms are replaced the effective contact potentials [47,48]. The physical argument for this replacement is that the detailed structure of the potential U is not resolved at the scale of the typical de Broglie wavelength associated with very low collision energies. Although the mathematical form of a contact potential does not lead to a well defined scattering problem, it can nevertheless give sensible results within theories which treat the interaction perturbatively, once issues with ultraviolent divergences are cured [49,50]. In particular we mention the description of damped oscillations in a mixed condensate [27,28].

However, since the effective contact potentials eliminate the details of the real potential, some physical quantities, such as the kinetic and interaction energies of the gas [40] cannot be predicted. Similarly, the presence of many bound levels in the potential is not directly taken into account, whereas these bound levels can play an important role in the dynamics of photoassociation with chirped laser pulses [32,33]. For these strongly time-dependent situations the details of the potentials will be important, since their structure is explored over a wide range of internuclear separations. This motivates us to formulate a theory which does not rely on the contact interaction assumption.

C. Theory with realistic interactions

Realistic interaction potentials $U(r)$ may have a deep well and a strong repulsive wall at short interatomic separations r. Because of these features, perturbative treatments like the Born approximation are inadequate. For instance, the "Born" scattering length of the potential U

$$a_{Born}[U]=\frac{m}{4\pi\hbar^2}\int d^3\mathbf{r}\,U(r) \tag{5}$$

is a poor approximation of the actual scattering length a. In fact, because of the repulsive wall, most potentials are singular at $r=0$ so they cannot be integrated over space. As a result, a_{Born} diverges in principle. In order to obtain finite results we need to start from the exact expression for the scattering length

$$a[U]=\frac{m}{4\pi\hbar^2}\int d^3\mathbf{r}\,U(r)\varphi_{2B}(r), \tag{6}$$

where φ_{2B} is the solution of the two-body Schrödinger equation at zero energy: $\left[-\frac{\hbar^2\nabla^2}{m}+U(r)\right]\varphi_{2B}(\mathbf{r})=0$ and is normalized to be asymptotically equal to 1. The deviations from one of the wave function φ_{2B} represent the correlations induced by the potential. In particular, because of the strong repulsive wall, $\varphi_{2B}(r)$ vanishes for r less than a few Bohr radii as it is nearly impossible to find two atoms in this region. As a result, the integrand $U(r)\varphi_{2B}(r)$ in Eq. (6) is regular for short r, which leads to a finite $a[U]$. Interestingly, Eq. (6) can be seen as the perturbative expression (5) where the "bare" potential is replaced by a new effective potential $\mathcal{U}_{2B}(r)=U(r)\varphi_{2B}(r)$.

In a well-defined many-body theory we also expect that when the potential appears in an equation it is always multiplied by many-body correlation functions φ_{MB} which go to zero for short interatomic separations and are equal to 1 at large separations [39,51,52]. This leads to effective regularized potentials $\mathcal{U}_{MB}(r)=U(r)\varphi_{MB}(r)$. In the following, we will consider two sets of equations which comply to this regularization requirement. The many-body correlation will be given by

$$\varphi_{MB}(r)=\frac{\Phi_g(r)}{\Psi\Psi} \tag{7}$$

i.e., the pair wave function normalized to its asymptotic value, which we call the reduced pair wave function.

1. First-order cumulant (FOC) approximation

A systematic method to truncate the infinite set of equations of the many-body problem, named the "cumulant method," has been proposed by Fricke [37]. This method redefines the different quantum averages in terms of quantities called noncommutative cumulants, which are constructed in such a way that for a sufficiently weak interaction, they decrease towards zero with an increasing order. Therefore, neglecting all the cumulants of order larger than a given order n gives a consistent truncated set of equations for a system close to the ideal gas. However, this assumption might fail for realistic interactions which can induce strong correlations at short distances. To extend the validity of the cumulant method, Köhler and Burnett [34] have devised a modified version of the truncation scheme where the free evolution of the cumulants of order $n+1$ and $n+2$ is taken into account. This regularizes the interaction in the first n equations, in a way similar to what we discussed in the previous paragraph. As a consequence, this extended cumulant method is technically applicable to realistic potentials, although it has been used so far only with effective separable potentials in the context of atomic and molecular condensates [36,53].

In the case of a two channel problem, the relevant cumulants up to second order are Ψ, $\Phi_g'=\Phi_g-\Psi\Psi$, Φ_e, and R_g'. The extended cumulant method to first order leads to the coupled equations [53]

$$i\hbar\frac{\partial\Psi(t)}{\partial t} = M(t)\Psi(t), \tag{8}$$

$$i\hbar\frac{\partial}{\partial t}\begin{pmatrix}\Phi_g(r,t)\\ \Phi_e(r,t)\end{pmatrix} = [\mathbf{H}^{(2)}(r,t)]\begin{pmatrix}\Phi_g(r,t)\\ \Phi_e(r,t)\end{pmatrix} + 2M(t)\begin{pmatrix}\Psi^2(t)\\ 0\end{pmatrix}, \tag{9}$$

where we introduced the mean-field potential

$$M(t) = \frac{1}{\Psi(t)}\int d^3\mathbf{r}\Psi^*(t)[U_g(r)\Phi_g(r,t) + W(r,t)\Phi_e(r,t)]. \tag{10}$$

This potential can be cast in the form of the usual Gross-Pitaevskiĭ mean-field potential by defining a time-dependent mean-field scattering length

$$a_M(t) = M(t)\frac{m}{4\pi\hbar^2|\Psi(t)|^2}. \tag{11}$$

We note that the potential U_g is always multiplied by the regularizing pair wave function Φ_g in Eqs. (8) and (9).

Besides these dynamical equations, there is a conservation relation

$$\rho = \rho_g(t) + \rho'_g(t) + \rho_e(t), \tag{12}$$

where ρ is the total density, $\rho_g(t)=|\Psi(t)|^2$ is the density of condensate atoms in the initial channel, $\rho'_g(t)=R'(0,t)$ is the density of noncondensate atoms in the initial channel, and $\rho_e=4\pi\int|\Phi_e(r,t)|^2r^2dr$ is the density of atoms in the excited (molecular) channel. The first-order cumulant equations imply an "approximate Bogoliubov relation" [34,54]

$$R'(r,t) = \int d^3\mathbf{z}\Phi'^*_g(\mathbf{z},t)\Phi'_g(\mathbf{r}-\mathbf{z},t), \tag{13}$$

which links the (ground channel) noncondensate density matrix to the correlated part of the component of the pair wave function in the ground channel. This relation is extremely useful as it guarantees in principle the positivity of the noncondensate density matrix R', so that all occupation numbers of the noncondensate modes have to remain positive.

However, we should remark that the initial noncondensate fraction predicted by Eq. (13) is generally an overestimation, because of the inappropriate long-range behavior of Φ within the first-order approximation. Indeed, the stationary solutions of Eqs. (8) and (9) show that $\Phi\propto 1-a_M/r$ at large distances r (which is known to be incorrect from the Bogoliubov theory, see Ref. [49]), so that the right-hand side of Eq. (13) diverges. When calculations are performed within a box, the results depend on the size of the box in an unphysical way. Therefore one should discard the initial number of noncondensate atoms as meaningless, considering only the subsequent variations. Note however that these variations may become negative, which would be interpreted as negative occupation numbers.

2. Reduced pair wave (RPW) approximation

We now consider another approximation introduced in our previous work [38] (see assumption *H*2), which we refer to as the "reduced pair wave approximation". The idea is to consider that the reduced pair wave function φ_{MB} defined in Eq. (7) should be close to the two-body wave function φ_{2B}. By assuming that it obeys exactly the two-body Schrödinger equation, we obtain the following set of equations:

$$i\hbar\frac{\partial\Psi(t)}{\partial t} = M(t)\Psi(t), \tag{14}$$

$$i\hbar\frac{\partial}{\partial t}\begin{pmatrix}\Phi_g(r,t)\\ \Phi_e(r,t)\end{pmatrix} = \left[\mathbf{H}^{(2)}(r,t) + \begin{pmatrix}2M(t) & 0\\ 0 & 0\end{pmatrix}\right]\begin{pmatrix}\Phi_g(r,t)\\ \Phi_e(r,t)\end{pmatrix}, \tag{15}$$

with the mean field $M(t)$ still defined by Eq. (10). These equations are very similar to the first-order cumulant equations. The only difference is that the mean-field term $M(t)$ now appears as a potential in Eq. (15) instead of a source term as in Eq. (9). The physical interpretation is that a pair of condensate atoms "feels" the mean-field potential not only at large interatomic separations, but also at shorter distances where the two atoms are correlated.

The conservation relation (12) still holds, but the approximate Bogoliubov relation (13) is no longer valid. We have not found an alternative relation in this approximation which would guarantee the positivity of the noncondensate occupation numbers.

D. Introduction of the spontaneous emission

When a pair of atoms in a confining trap is photoassociated, populating a bound vibrational level of the potential $U_e(r)$, the excited molecule has a finite lifetime and decays back to the ground electronic state by spontaneous emission of a photon. Most often, the final state is a continuum level of the ground potential $U_g(r)$, where the pair of atoms has enough energy to escape the trap. In some cases, the radiative transition populates a bound level of $U_g(r)$, leading to the formation of stable molecules [43,55].

In the previous equations, decay by spontaneous emission is not considered. Assuming that it is mainly a loss phenomenon, it can be accounted for by adding an imaginary term to the excited potential $U_e(r)$

$$U_e(r) \to U_e(r) - i\frac{\hbar\gamma}{2}, \tag{16}$$

where $1/\gamma$ is the radiative lifetime of the bound levels in the excited potential (we have assumed the dipole moment to be r independent). The component of the pair wave function in the closed channel therefore contains an exponentially decreasing factor: as a result, the total density (12) is no longer conserved during the time evolution.

IV. MEAN-FIELD EQUATIONS AND ROGUE DISSOCIATION

As a general rule, the coupled mean-field (Gross-Pitaevskiĭ) equations of Ref. [25] are retrieved from both approximations when the pair dynamics can be elimi-

nated adiabatically with respect to the one-body dynamics [38]. However the adiabaticity condition given in Paper I [38] (merely comparing the coupling constants in the equations) has to be refined. We give here a more relevant condition, related to the *rogue dissociation* analysis of Ref. [56].

Let us first assume that only one excited molecular level is resonant. In this case, we call δ the detuning of the laser from this molecular level (see Fig. 1). One can write $\Phi_e(r,t) \approx \sqrt{2}\Psi_m(t)\varphi_m(r)$, where $\varphi_m(r)$ is the volume-normalized wave function for the relative motion in this resonant molecular level and $\Psi_m(t)$ is the (here uniform) center-of-mass wave function corresponding to a molecular condensate. With this normalization, $|\Psi_m|^2$ is the density of molecules.

Then, the crucial point is to write the correlation in the pair wave function as a sum of an adiabatic correlation and a dynamic correlation

$$\Phi_g(r,t) = \Psi^2(t) + \Phi_g^{ad}(r,t) + \Phi_g^{dyn}(r,t) = \Psi^2(t)[1 + \varphi_g^{ad}(r,t) + \varphi_g^{dyn}(r,t)].$$

The adiabatic part is found by setting Φ_g^{dyn} and $\frac{\partial}{\partial t}\Phi_g^{ad}$ to zero in Eq. (9) or φ_g^{dyn} and $\frac{\partial}{\partial t}\varphi_g^{ad}$ to zero in Eq. (15). We can then expand the correlation in terms of the scattering states $|\varphi_{\mathbf{k}}\rangle$ of the ground potential U_g

$$\Phi_g(r,t) = \Psi^2(t) + \int \frac{d^3\mathbf{k}}{(2\pi)^3}[C_{\mathbf{k}}^{ad}(t) + C_{\mathbf{k}}^{dyn}(t)]\varphi_{\mathbf{k}}(r)$$

with the normalization $\langle\varphi_{\mathbf{k}}|\varphi_{\mathbf{q}}\rangle = (2\pi)^3\delta^3(\mathbf{k}-\mathbf{q})$ [62]. We find

$$C_{\mathbf{k}}^{ad}(t) = -\frac{m}{\hbar^2 k^2}(g_{\mathbf{k}}\Psi^2 + w_{\mathbf{k}}\Psi_m). \tag{17}$$

Eliminating this adiabatic part in Eqs. (8) and (9) or (14) and (9) leads to the terms of the mean-field equations [38]. The equations for Ψ and Ψ_m then read

$$i\hbar\dot{\Psi} = \Psi^*\left[\left(g_0\Psi^2 + \int \frac{d^3\mathbf{k}}{(2\pi)^3}g_{\mathbf{k}}C_{\mathbf{k}}^{dyn}\right) + w\Psi_m\right], \tag{18}$$

$$i\hbar\dot{\Psi}_m = \hbar\left(\delta' - i\frac{\gamma}{2}\right)\Psi_m + \frac{1}{2}\left(w_0\Psi^2 + \int \frac{d^3\mathbf{k}}{(2\pi)^3}w_{\mathbf{k}}C_{\mathbf{k}}^{dyn}\right) \tag{19}$$

where

(i) $g_{\mathbf{k}} = \int d^3r U(r)\varphi_{\mathbf{k}}(r)$ is the atom-atom scattering coupling constant (in particular $g_0 = \frac{4\pi\hbar^2 a}{m}$)

(ii) $w_{\mathbf{k}} = \sqrt{2}\langle\varphi_{\mathbf{k}}|W|\varphi_m\rangle$ is the atom-molecule coupling constant

(iii) $\delta' = \delta + E_{self}$ is the detuning shifted by the self-energy of the molecules

The equation for the dynamic correlation in the first-order cumulant approximation is

$$i\hbar\dot{C}_{\mathbf{k}}^{dyn} = \frac{\hbar^2\mathbf{k}^2}{m}C_{\mathbf{k}}^{dyn} - i\hbar\dot{C}_{\mathbf{k}}^{ad}, \tag{20}$$

and in the reduced pair wave approximation

$$i\hbar\dot{c}_{\mathbf{k}}^{dyn} = \frac{\hbar^2\mathbf{k}^2}{m}c_{\mathbf{k}}^{dyn} - i\hbar\dot{c}_{\mathbf{k}}^{ad}, \tag{21}$$

with $c_{\mathbf{k}} = C_{\mathbf{k}}/\Psi^2$. As long as the momentum distribution of $C_{\mathbf{k}}^{dyn}$ lies in the Wigner's threshold regime, we can make the simplification: $g_{\mathbf{k}} \approx g_0$ and $w_{\mathbf{k}} \approx w_0$. Note that this approximation does not lead to any ultraviolet divergence, because we have eliminated the adiabatic correlation beforehand. Such an approximation, reminiscent of the use of a contact potential, would have given rise to ultraviolet divergences if we had made it in the original equations (8) and (9) or (14) and (9).

It is now clear from Eqs. (18) and (19), that when the dynamic correlation $C_{\mathbf{k}}^{dyn}$ is negligible, one gets the Gross-Pitaevskiĭ equations of Ref. [25]

$$i\hbar\dot{\Psi} = g_0|\Psi|^2\Psi + w_0\Psi^*\Psi_m, \tag{22}$$

$$i\hbar\dot{\Psi}_m = \hbar\left(\delta' - i\frac{\gamma}{2}\right)\Psi_m + \frac{1}{2}w_0\Psi^2. \tag{23}$$

The mean-field approximation will break down when the dynamic correlation is not negligible any more. This means that molecules break into pairs of atoms which will contribute to the noncondensate fraction instead of the condensate fraction. From Eqs. (18) and (19) we see that such *rogue dissociation* [56] can be neglected as long as

$$\left|\int \frac{d^3\mathbf{k}}{(2\pi)^3}C_{\mathbf{k}}^{dyn}\right| \ll |\Psi^2|. \tag{24}$$

To give a more explicit condition, we first have to make a distinction between two different regimes of Eqs. (22) and (23).

A. The adiabatic regime

We consider the limit when $|i\hbar\dot{\Psi}_m| \ll |\frac{1}{2}w_0\Psi^2|$. In this case, Ψ_m can be eliminated adiabatically, so that

$$\Psi_m \approx -\frac{w_0}{2\hbar\left(\delta' - i\frac{\gamma}{2}\right)}\Psi^2 \tag{25}$$

and

$$i\hbar\dot{\Psi} \approx \left[g - \frac{w_0^2}{2\hbar\left(\delta' - i\frac{\gamma}{2}\right)}\right]|\Psi|^2\Psi \equiv \frac{4\pi\hbar^2 a_M}{m}|\Psi|^2\Psi. \tag{26}$$

In this regime, the coupled equations reduce to a single Gross-Pitaevskiĭ equation [25,28] where the mean-field scattering length a_M corresponds to the modified scattering length

$$A = a + a_{\text{opt}} + ib_{\text{opt}}$$

given by the two-body theory of the resonance [16,17]. Therefore, most physical properties can be described by the usual two-body theory. For instance, Eq. (26) implies that the

atomic density $\rho_g = |\Psi|^2$ follows a simple rate equation:

$$\dot{\rho}_g = -\frac{8\pi\hbar b_{\text{opt}}}{m}\rho_g^2, \tag{27}$$

and using (17) and (25), one can calculate the pair wave function and find the usual asymptotic behavior

$$\Phi_g(r,t) \xrightarrow[r\to\infty]{} \Psi^2(t)\left(1-\frac{a_M}{r}\right). \tag{28}$$

As a matter of fact, the molecular field Ψ_m scales as ρ in this regime: it is merely a two-body field playing the role of an intermediate state during the collision process. Using (25) and (26), we find that the condition $|i\hbar\dot{\Psi}_m| \ll |\frac{1}{2}w_0\Psi^2|$ is satisfied whenever

$$\hbar\left|\delta' + i\frac{\gamma}{2}\right| \gg w_0\sqrt{\rho}, \quad 2g\rho. \tag{29}$$

This corresponds to the *off-resonant regime* of Ref. [25]: the detuning and the spontaneous emission are large with respect to the coherent couplings.

B. The coherent regime

On the other hand, we may consider the limit $|\hbar(\delta' - i\frac{\gamma}{2})\Psi_m| \ll |\frac{1}{2}w_0\Psi^2|$ and $|g_0|\Psi|^2\Psi| \ll |w_0\Psi^*\Psi_m|$. In this case, the solutions of Eqs. (22) and (23) for an initially all atomic system are

$$\Psi \approx \sqrt{\rho}/\cosh(w_0\sqrt{\rho}t),$$

$$\Psi_m \approx -i\sqrt{\rho}\tanh(w_0\sqrt{\rho}t).$$

There is a coherent conversion between atoms and molecules. In this regime, Ψ_m scales as $\sqrt{\rho}$ and plays the role of a one-body field, i.e., a molecular condensate in its own right. As a result, the system cannot be described by a two-body theory any more. For instance, the pair wave function is still of the form (28), but the mean-field scattering length a_M is now a time-dependent quantity $a - iL\sinh(2w_0\sqrt{\rho}t)$ where

$$L = \frac{m}{4\pi\hbar}\frac{w_0}{2\sqrt{\rho}}$$

is a many-body length which depends on the density. This means that the density of atoms does not follow a rate equation.

We find that this coherent regime occurs when

$$w_0\sqrt{\rho} \gg \hbar\left|\delta' + i\frac{\gamma}{2}\right|, \quad 2g\rho. \tag{30}$$

In practice, while it is possible to set the detuning to zero by varying the laser frequency, the spontaneous decay γ is fixed by the molecular level of the system. Spontaneous emission in alkali systems, and loss processes in general, make it very difficult to reach the coherence condition (30) with realistic densities and laser intensites. For this reason, photoassociation experiments in condensates so far [20,41,57] have been confined to the adiabatic regime (29), and can be described simply by two-body theories.

However, we made some estimates which indicate that photoassociation for weakly allowed transitions, such as those found in alkaline-earth dimers, would lead to the coherent regime. The reason is that spontaneous emission scales as the square of the dipole moment whereas the coherent coupling $w_0\sqrt{\rho}$ only scales as the dipole moment.

C. Rogue dissociation

In the coherent regime, which is the regime originally investigated in Ref. [56], the relevant energy scale set by the dynamics is $\hbar\Omega = w_0\sqrt{\rho}$ defining the coherent Rabi frequency $\Omega/2\pi$. As a result, Eq. (20) or (21) can be made dimensionless using the characteristic time $\tau = \Omega^{-1}$ and length $\xi = \sqrt{\hbar/m\Omega} = (4\pi L\rho)^{-1/2}$. Since $|\Psi|^2 \sim \rho$ and $|C_{\mathbf{k}}^{dyn}| \sim 1$, the rogue dissociation condition (24) can be written

$$(\rho\xi^3)^{-1} = \left(\frac{\hbar\Omega}{\frac{\hbar^2\rho^{2/3}}{m}}\right)^{3/2} = [(4\pi L)^3\rho]^{1/2} \ll 2\pi^2. \tag{31}$$

This condition was presented in Javanainen and Mackie's work [56].

Similarly, in the adiabatic regime, the relevant energy scale is $\hbar\Gamma = w_0^2\rho/\sqrt{\delta'^2 + (\gamma/2)^2}$ corresponding to the mean field energy $\hbar\Gamma = \frac{4\pi\hbar^2|A|}{m}\rho$. Equation (20) or (21) can be made dimensionless using the characteristic time $\tau_0 = \Gamma^{-1}$ and length $\xi_0 = \sqrt{\hbar/m\Gamma} = (4\pi|A|\rho)^{-1/2}$ (note that this is the usual healing length), and the rogue dissociation condition is now

$$(\rho\xi_0^3)^{-1} = \left(\frac{\hbar\Gamma}{\frac{\hbar^2\rho^{2/3}}{m}}\right)^{3/2} = [(4\pi|A|)^3\rho]^{1/2} \ll 2\pi^2. \tag{32}$$

Both conditions (31) and (32) can be written as $\sqrt{\rho a_M^3} \ll 1$ which is a straightforward generalization of the usual condition $\sqrt{\rho a^3} \ll 1$ for the validity of the Gross-Pitaevskiĭ equation. This can be interpreted as follows: rogue dissociation occurs when the average spacing $\rho^{-1/3}$ between the atoms becomes of the order of the typical length associated to the adiabatic correlation, either A in the adiabatic regime, or L in the coherent regime. However, there is a fundamental difference. A is the modified scattering length, a two-body quantity independent of the density; in the adiabatic regime, one can thus reach the rogue dissociation regime by increasing the density, so that the average spacing between the atoms becomes of the order of A. The mean-field equations are therefore valid at *low density* in the adiabatic regime. On the other hand, in the coherent regime, the many-body length L decreases with density, and more rapidly than the average spacing between the atoms. As a result, one should decrease the density to observe rogue dissociation. The mean-field equations are therefore valid at *high density* in the coherent regime. An overview of the different regimes and conditions is given in Fig. 2.

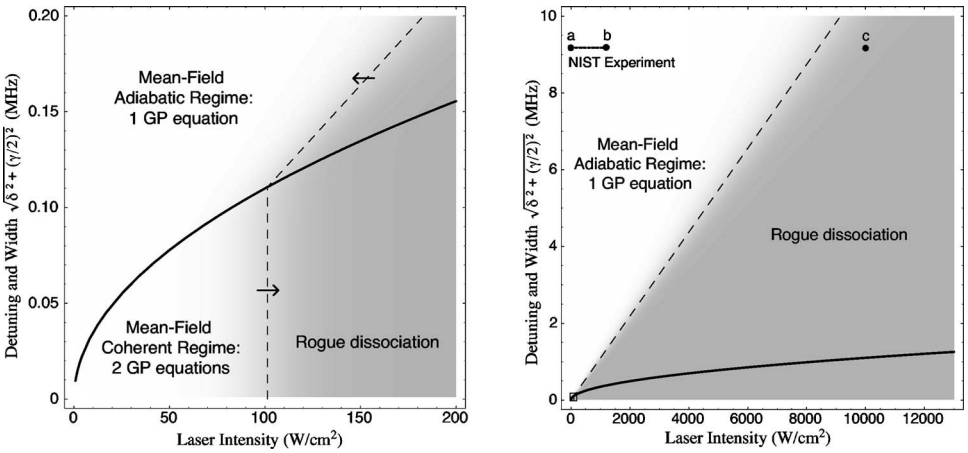

FIG. 2. Different regimes of photoassociation in a condensate, as a function of laser intensity and the combined effect of detuning and spontaneous emission. These graphs correspond to the sodium resonance described in Sec. VI A, for a density of 4×10^{14} atoms/cm^3, but spontaneous emission is taken as a free parameter. Left panel: the solid line is the limit between the adiabatic regime and the coherent regime of the mean-field equations (22) and (23). The mean-field approximation is valid in the white areas, and rogue dissociation occurs in the shaded areas. The vertical dashed lines corresponds to the left hand side of (31) being equal to π^2 and the oblique dashed line corresponds to the left hand side of (32) being equal to π^2. The arrows indicate how these lines move when the density is increased. Right panel: larger view showing the experimental investigation of Ref. [41] (from dot *a* to dot *b*) where the spontaneous emission parameter $\gamma/2$ is equal to $2\pi\times9.18$ MHz; dot *c* corresponds to the condition of our numerical investigation described in Sec. VI C.

V. NUMERICAL METHODS AND CALCULATIONS

We now turn to the numerical resolution of the time-dependent equations (8), (9), (14), and (15). The main difficulty is that they describe simultaneously the microscopic dynamics, with short characteristic times, and the macroscopic dynamics, with longer ones. At each time step, the mean field $M(t)$ and the mean-field scattering length $a_M(t)$ must be determined through Eqs. (10) and (11), from the two components of the pair wave function $\Phi_g(r,t)$ and $\Phi_e(r,t)$ and from the condensate wave function $\Psi(t)$. Then the mean field influences the evolution of the three wave functions in the coupled equations (8) and (9) or (14) and (15). Note that in previous calculations based on the cumulant equations [53], the use of a nonlocal, separable potential made it possible to first perform an independent integration of the two-body equation (15), then inject the results into the condensate equation to solve a non-Markovian nonlinear Schrödinger equation. This simplifying procedure is not implemented in the present paper where we use the same realistic potentials in both approaches.

The pair wave functions are represented on a grid, using a mapping procedure where the grid steps are adjusted to the local de Broglie wavelengths [58] in the two potentials, choosing the smallest of the two values at a given r. The short range oscillations are thus described with a dense grid and the long range behavior with a diffuse one. Typical value of the grid length L is $200\,000a_0$. The whole set of equations, either (8) and (9) or (14) and (15) are then solved, using the standard Crank-Nicholson method [59] for the propagation in time. The solutions at $t=0$ are chosen as stationary solutions for the open (ground) channel, when no laser coupling is present.

A. Initial state in the first-order cumulant approximation

Stationary solutions of Eqs. (8) and (9) are given by

$$\bar{\Psi} = \sqrt{\bar{\rho}_g}, \tag{33}$$

$$\begin{pmatrix} \bar{\Phi}_g(r,t) \\ \bar{\Phi}_e(r,t) \end{pmatrix} = -(\mathbf{H}^{(2)}(r,t) - 2\mu)^{-1} 2\mu \begin{pmatrix} \bar{\rho}_g \\ 0 \end{pmatrix}, \tag{34}$$

where $\bar{\rho}_g$ is the initial condensate density, and $\mu=\bar{M}$ is the chemical potential (equal to the initial mean field energy in the present case). When the laser is initially off, the coupling term W in $\mathbf{H}^{(2)}$ is zero. To compute (33) and (34), we start from a given value for the condensate density $\bar{\rho}_g$ and a guess value for μ. We determine the pair wave function from (34) by performing a matrix inversion. This gives a new value of the mean field through Eq. (10), and the procedure is iterated until convergence is reached for μ. It can be readily seen that when the chemical potential matches one of the Hamiltonian's eigenvalues, the matrix is singular and the solution shows an unphysical resonance of the mean-field scattering length. Theoretically, this can be fixed in the continuum limit [54], but the difficulty remains in a numerical calculation and is illustrated in Fig. 3. Between the resonances the mean-field scattering length is essentially equal to the expected scattering length of the two-atom system. We therefore choose an initial density that is both close to the experimental value and such that the mean-field scattering length does lie in between the resonances.

B. Initial state in the reduced pair wave approximation

Stationary solutions of Eqs. (14) and (15) are obtained by solving

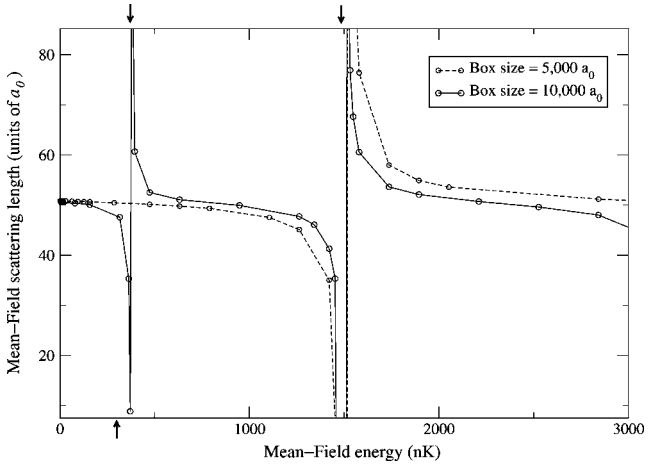

FIG. 3. Mean-field scattering length as defined from Eqs. (10) and (11), calculated from the stationary solution (33) and (34) of the first-order cumulant equations, as a function of the mean-field energy. The numerical calculations shown here correspond to the case of a sodium condensate without any photoassociation laser ($W=0$), and are performed within a square box of width $d=10\,000a_0$ (solid lines) or $d=5\,000a_0$ (dashed line). The position of the first two levels of the wider box are indicated by arrows on the upper horizontal axis, the second one coinciding with the first level of the $d=5\,000$ box. As explained in the text, the mean-field scattering length has an unphysical divergence each time the mean-field energy coincides with an energy level of the box. The latter depend on the arbitrary size the box; in our calculations, this size can typically go up to $200\,000a_0$, which increases the number of resonances. The typical mean-field energy in the experiment of Ref. [41] is about 6 kHz$\approx$300 nK, and indicated by an arrow on the lower horizontal axis.

$$\bar{\Psi} = \sqrt{\bar{\rho}_g}, \tag{35}$$

$$0 = \left[\mathbf{H}^{(2)}(r,t) - \begin{pmatrix} 0 & 0 \\ 0 & 2\mu \end{pmatrix} \right] \begin{pmatrix} \bar{\Phi}_g(r,t) \\ \bar{\Phi}_e(r,t) \end{pmatrix}. \tag{36}$$

The two-component function $(\bar{\Phi}_g, \bar{\Phi}_e)$ is therefore the zero energy stationary solution of the two-channel problem, the potential U_e being shifted down by twice the chemical potential. This means that the energy of the optically induced Feshbach resonance is shifted by the mean-field energy of the condensate atoms, even though the collision energy is nearly zero. Apart from this shift, the mean-field scattering length is equal to the usual two-body scattering length and is free of the resonance problem in the FOC approximation. This is because an extra short-range correlation is taken into account with respect to the FOC approximation (see Appendix).

To determine eigenfunctions of Eq. (36) we propagate Eq. (15) in imaginary time with the Crank-Nicholson scheme [59]. The finite value of the time step value acts as an energy filter, which selects the zero energy scattering state in a few steps.

C. Accuracy check: computation of the scattering length

Checks on the macroscopic dynamics can be performed by comparing with the mean-field equations (22) and (23) when rogue dissociation is negligible (see below). As for the microscopic dynamics, we have to ensure that the mean-field scattering length (11), deduced from the integral expression (10), is computed accurately enough at each time step. To that purpose, we have solved the stationary version of the two-body equations (2) and extracted the phase shift of the continuum wave function in the open channel from its asymptotic behavior. The scattering length can be deduced by extrapolation to zero collision energy. In Fig. 4, we compare the scattering length computed by this method, and the mean-field scattering length given by Eq. (10). One can see from the excellent agreement that the latter is indeed accurately computed in the stationary case.

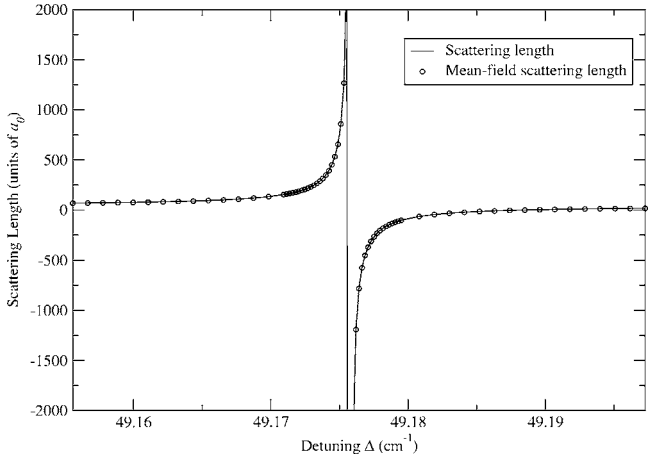

FIG. 4. Optically induced Feshbach resonance: variation of the sodium scattering length as a function of the detuning of the photoassociation laser in the vicinity of the $v=135$, $J=1$ resonance [41], for a laser intensity of 15 kW/cm^2, and a variable detuning Δ relative to the D_1 atomic resonance line. Spontaneous emission is not included in these calculations. Solid line: scattering length determined by phase shift from two-atom calculations. Dots: mean-field scattering length as defined by Eqs. (10) and (11), calculated from the stationary states in the reduced pair wave approximation, see Eqs. (35) and (36).

VI. APPLICATION: PHOTOASSOCIATION IN A SODIUM CONDENSATE

A. Experimental conditions of the NIST experiment

The chosen example starts from the photoassociation experiment in NIST [41], where a condensate of sodium atoms is illuminated by a cw laser of intensity I varying from 0.14 to 1.20 kW/cm^2. The peak density is about 4×10^{14} atoms/cm^3. The frequency (16 913.37 cm^{-1}) is chosen at resonance with the $J=1$, $v=135$ vibrational level in the 0_u^+ $(3S+3P_{1/2})$ potential curve of Na_2. The detuning of the photoassociation laser relative to the $\mathbf{D}_1$ resonance line is rather large (43 cm^{-1}), and corresponds to the binding energy of the $v=135$ level. The molecules formed in the excited electronic state have a natural width $\gamma=2\pi\times18.38$ MHz due to spontaneous emission.

Previous estimations [41] based on criterion (31) [56] predicted that these experimental conditions should lead to

rogue dissociation, as $(2\pi^2\rho\xi^3)^{-1}\approx 3.2$ for $I=1.2$ kW/cm^2. However, this criterion is relevant only in the coherent regime. According to the analysis of Sec. IV, the experiment is actually in the adiabatic regime (see Fig. 2), as $2\Omega/\gamma \sim 0.04$. Therefore, the relevant criterion is (32). As $(2\pi^2\rho\xi_0^3)^{-1}\approx 0.03$ for $I=1.2$ kW/cm^2, one concludes that no rogue dissociation should occur and the mean-field approximation should be valid, which is consistent with the experimental observation. However, if the intensity can be increased up to 10 kW/cm^2, then $(2\pi^2\rho\xi_0^3)^{-1}\approx 0.6$ and rogue dissociation should occur (see Fig. 2). We therefore present numerical calculations simulating the experiment in this high-intensity regime to see the effects of rogue dissociation. Calculations in similar conditions were done by Gasenzer [53] using the first-order cumulant equations with separable potentials.

B. Parameters of the calculations

For these calculations, the potentials curves for the ground state of Na_2 $X\,^1\Sigma_g^+$ and $0_u^+(3s+3p_{1/2})$ have been taken from Ref. [60]. The ground state potential is chosen so that the scattering length is $54.9a_0$, as in Gasenzer's work [53]. Hyperfine structure is not included, and the last bound level has a binding energy of 317.78 MHz ($\sim 10^{-2}$ cm^{-1}). In the excited curve, the level $v=135$ is bound by 49.23 cm^{-1}, the two neighboring levels being $v=134$ at -52.95 cm^{-1} and $v=136$ at -45.757 cm^{-1}. The spontaneous emission term (16) for this excited state is set to $\gamma=2\pi\times 18.36$ MHz to match the experiment [41].

The dipole moment matrix element is taken as $D=2$, assuming linear polarization of the laser, neglecting r dependence, and deducing the atomic lifetime from the long range coefficient $C_3=6.128$ of Marinescu and Dalgarno [61]. The coupling term W in Eq. (2) is therefore linked to the intensity I by $W=\sqrt{2I/(c\varepsilon_0)}$.

We model the cw laser as follows: the intensity starts from zero and is turned on linearly $[I_b(t)=I\times t/T;\ t\leqslant T]$ to become constant and equal to I after $t=T=0.5$ μs. This value of T, previously used in the calculations by Gasenzer [53], corresponds to the typical rise and fall-off times of the laser in the experiment of Ref. [41]. Starting from a pure sodium condensate, with a density $\rho(t=0)=\rho_g(t=0)$, and therefore assuming $\rho'(t=0)=\rho_e(t=0)=0$, we have solved the coupled equations (8), (9), (14), and (15) as well as the mean-field equations (22) and (23). From these calculations, we obtain the time variation of the relative number of condensate atoms

$$\alpha_g(t)=\rho_g(t)/\rho(0);\quad \alpha_g(0)=1, \tag{37}$$

of noncondensate atoms in the open channel

$$\alpha'_g(t)=\rho'_g(t)/\rho(0);\quad \alpha'_g(0)=0, \tag{38}$$

and the relative number of atoms in the closed channel

$$\alpha_e(t)=\rho_e(t)/\rho(0)=2\beta_e(t);\quad \beta_e(0)=0, \tag{39}$$

which is twice the relative number of photoassociated molecules $\beta_e(t)$. The remaining fraction $1-\alpha_g-\alpha'_g-\alpha_e$ corresponds to photoassociated molecules that have been deexcited by spontaneous emission, yielding either cold molecules in the ground state or pairs of "hot atoms" that usually leave the trap.

C. Results for high intensities

We first performed calculations for laser intensities I in the range of the experiment (from 140 to 1200 W/cm^2). The photoassociation dynamics on resonance is reported in Fig. 5, showing the condensate, noncondensate fractions, as well as the mean-field scattering length as a function of time. Here we are far from the rogue dissociation limit (see dots a and b in Fig. 2). As expected, the noncondensate fraction remains negligible and all approximations agree with the mean-field approximation.

Since we are in the adiabatic regime (see Fig.2 again), the mean-field approximation is consistent with the usual two-body theory. This can be seen in the left column of Fig. 8, where we plotted the photoassociation line shape, as well as the variation of the mean-field scattering length as a function of the frequency of the laser. The line shape presents no difference from the one predicted by two-body theory, nor does the mean-field scattering length from the optically modified scattering length of the two-body theory [16,17].

We then performed calculations for $I=10$ kW/cm^2. We are now in the rogue dissociation regime where deviations from the mean-field approximation are expected. The on-resonance dynamics is plotted in Fig. 6. We observe the following effects in both the FOC and RPW approximations:

(1) First, there is a significant final fractions of noncondensate atoms, which of course are ignored in the Gross-Pitaevskiĭ picture.

(2) Second, the decay of the condensate at short times is slower than the one predicted by the Gross-Pitaevskiĭ coupled equations.

These two effects arise from the dynamic correlation Φ_g^{dyn} discussed in Sec. IV, but have different interpretations.

1. Creation of correlated pairs

Let us first study how the noncondensate atoms are produced. This can be done by analyzing the ground state component of the pair wave function, illustrated in Fig. 7. We see that a strong maximum emerges in the wave function Φ_g around $55a_0$, which we identify with the presence of weakly bound molecules, corresponding to population of the last vibrational levels in the $X\,^1\Sigma_g^+$ potential. However, these bound states give a very small contribution to the fraction of noncondensate atoms and they disappear when the laser is turned off. They are in fact a near-resonance feature of the adiabatic correlation Φ_g^{ad} which is already explained by the stationary two-body theory.

The significant fraction of noncondensate atoms is explained by the appearance of waves in the pair wave function at larger distances (Fig. 7). In both FOC and RPW calculation, these waves are created at short distances as soon as the laser is turned on and then propagate in the outward direction, reaching distances where they are no longer affected by the laser coupling—they are not affected when the laser is switched off. This explains why the fraction of nonconden-

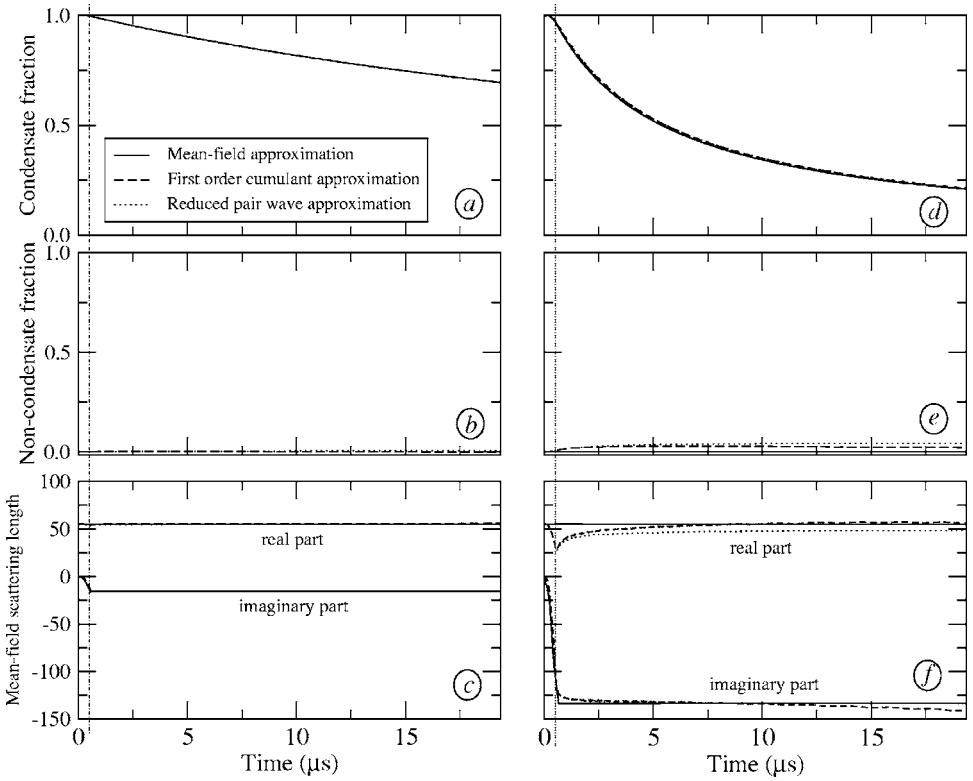

FIG. 5. On-resonance photoassociation dynamics for the $v=135$ level of Na_2 $A\,^1\Sigma_u^+$ using a cw laser of intensity (for $t>0.5$ μs) $I=140$ W/cm^2 (left column) and $I=1200$ W/cm^2 (right column). This corresponds to the adiabatic regime where all approximations reduce to the mean-field approximation and are consistent with usual two-body theory. Top panels (a) and (d): the decay of the condensate fraction $\alpha_g(t)$ is caused by spontaneous emission and dissociation of the photoassociated molecules into pairs of atoms which escape the trap. This decay is more rapid in panel (d), due to the larger intensity (1200 W/cm^2) of the photoassociation laser. Middle panels (b) and (e): time variation of the fraction of noncondensate ground state atoms $\alpha_g'(t)$, which remains negligible. Bottom panels (c) and (f): time variation of the real Re$[a(t)]$ and imaginary Im$[a(t)]$ part of the mean-field scattering length (in units of a_0).

sate atoms becomes mostly constant after 5 μs. Thus, these noncondensate atoms correspond to correlated pairs of free atoms with opposite momenta. Their typical kinetic energy is expected to be of the order of $\hbar\Gamma \sim 2\mu K$, which is consistent with the wavelength of the waves observed in the pair wave function. For weak trapping potentials, they may leave the system. Otherwise, one should treat the collisions between these correlated pairs and the condensate atoms in the presence of the laser field. However this goes beyond both the FOC and RPW approximations.

The appearance of the correlated pairs at high intensity has already been predicted in Gasenzer's work and it was shown that it leads to a saturation of the number of possible stable molecules formed by spontaneous emission [53]. However, it is worth noting that the formation of these pairs is a consequence of the fast rise ($T=0.5$ μs) of the laser intensity, and is most probably related to a two-body nonadiabatic effect—the waves also appear in a time-dependent two-body calculation. The right column of Fig. 6 shows the on-resonance dynamics when the laser intensity is raised more slowly for $T=16$ μs. We can see that the final fraction of noncondensate atoms is notably reduced in both approximations. This shows that the creation of correlated pairs is greatly sensitive to the way the laser is turned on. In contrast, the depletion of the condensate still shows a marked deviation from the mean-field prediction. We can then proceed with the discussion of this depletion, ignoring the noncondensate atoms.

2. Limitation of the decay rate

In all models, the decay rate of the condensate $K(t) = \frac{h}{m} 4|\mathrm{Im}[a_M(t)]|$ is proportional to the imaginary part of the mean-field scattering length, the latter being one fourth of the photoassociation characteristic length introduced in Ref. [41]. The imaginary part of the mean-field scattering is plotted in the bottom panels of Fig. 6. At short times, both the FOC and RPW approximations lead to the same rate, which is clearly smaller than the one predicted by the mean-field approximation. Such a limitation of the rate was already pointed out in the coherent regime [56], and also observed in the adiabatic regime [53].

Our interpretation is the following: because of the rogue dissociation, excited molecules are coupled back to the condensate through the dynamic correlation. This extra correlation reduces the efficiency of the coupling between the condensate and the excited molecules, thereby reducing the loss from the condensate. The fact that this effect does not depend on the way the laser is turned on suggests that it is a genuine many-body effect, namely the influence of the dynamics of the medium on the pair dynamics. We also note that the dynamic correlation responsible for this limitation of the rate

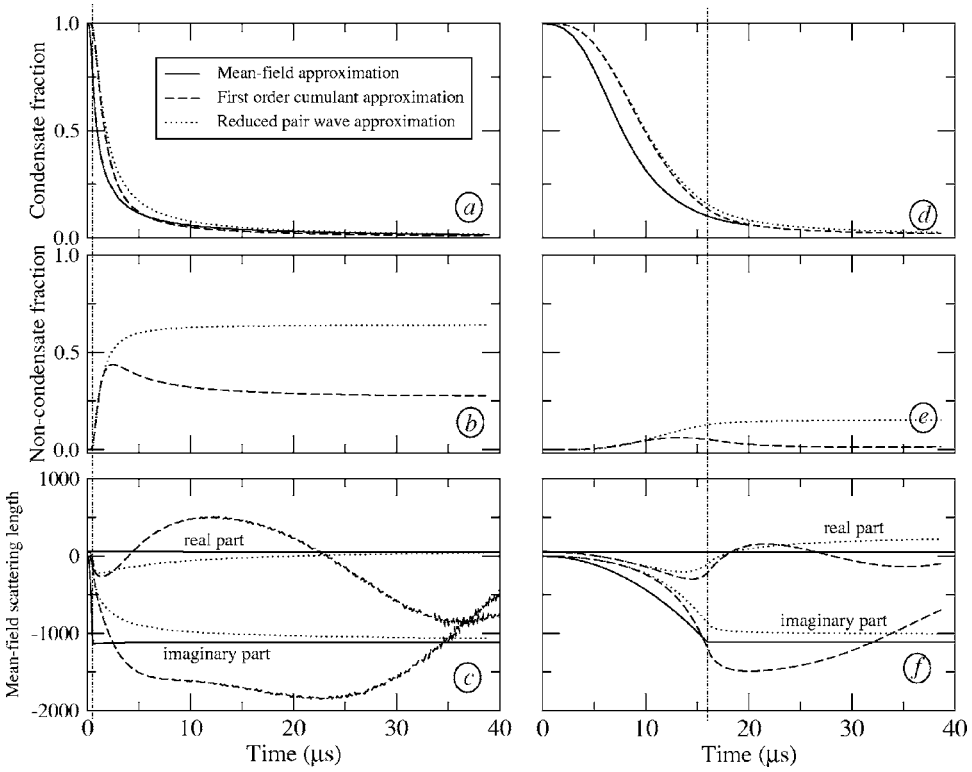

FIG. 6. Same as Fig. 5 for an intensity of 10 kW/cm^2. Left column corresponds to a rise time of the laser of 0.5 μs, whereas right column corresponds to a rise time of 16 μs (the end of the ramp is indicated by a dotted-dashed vertical line).

gives a very small contribution to the noncondensate atoms, unlike the part corresponding to the correlated free atoms. We suspect from Eqs. (18)–(21) that the Fourier transform of this correlation scales as $1/k^4$.

Note that at longer times in the reduced pair wave approximation, the rate (and more generally the mean-field scattering length) approaches the standard two-body rate (standard scattering length A). On the other hand, in the first-order cumulant approximation the rate finally exceeds the standard rate and starts oscillating. However, these differences are not so significant from the experimental point of view because they occur at a point where there are very few condensate atoms remaining in the system.

3. Symmetry of the line shape

The differences between the RPW and FOC approximations are more conspicuous in the line shape of the resonance, see right column of Fig. 8. In the RPW approximation the final condensate and noncondensate fractions are symmetric with respect to the resonance. On the other hand, in the FOC approximation the line shape becomes very asymmetric: on the "blue" side of the resonance (where the bare resonant state lies below the dressed threshold) the condensate is more depleted and more noncondensate atoms are produced than on the "red" side. We suspect that this asymmetry is due to the strong dependence of the scattering properties on the mean-field energy in the FOC approximation, as we saw in Sec. V A. Indeed, at high intensity the mean-field energy becomes large and positive on the blue side while it is large and negative on the red side. On the other hand, the scattering properties in the RPW approximation correspond mainly to those of the usual zero energy scattering problem.

Comparison of these predictions with experiment may not be straightforward. First, there are important experimental issues such as inhomogeneous broadenening to overcome at these high intensities [41]. Second, collisions between condensate and noncondensate atoms are neglected in both approximations. Furthermore, one has to keep in mind that the RPW approximation brings some correction to the FOC approximation, but only in an incomplete way (see Appendix). However, at a qualitative level, the symmetry of the experimental line shapes at these high intensities could show the relevance of this mean-field correction occurring at short interatomic distance.

4. Realistic potentials and cw lasers

Finally, we should note that our calculations using the FOC approximation with realistic potentials agree with Gasenzer's calculations which use a separable potential [53], except for times when the condensate fraction becomes negligible. This shows that no major improvement is brought by the details of the potential in these cw laser photoassociation calculations. Using the simplified equations (18)–(21) in this case would lead to similar results. In fact, since we have addressed only the adiabatic regime (see Fig. 2), only two equations would be sufficient, namely (18) and (20) or (18) and (21), as the molecular condensate Ψ_m can be eliminated adiabatically in these equations. Note that these equations are very similar to those of say, Ref. [56], but are free of any ultraviolet divergence or renormalization process as the adiabatic correlation have been eliminated from the equations in the first place.

In the more complex photoassociation processes involving pulsed lasers, the simplified equations are inadequate and

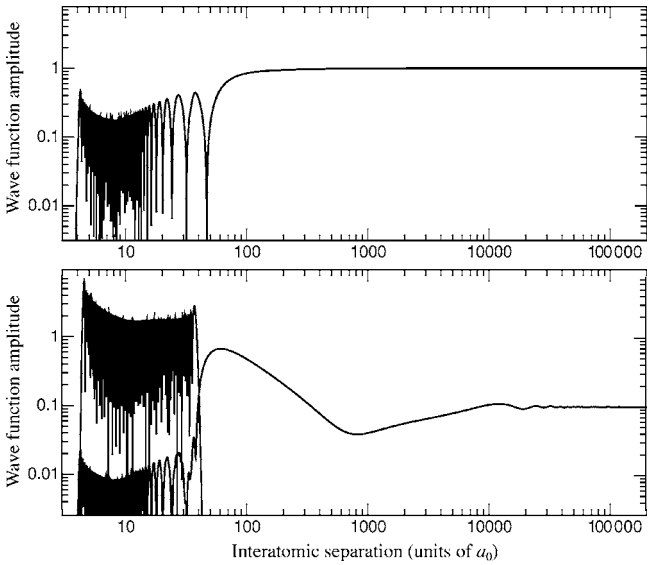

FIG. 7. Modulus of the two components $\phi_g(r)$ and $\phi_e(r)$ of the pair wave function in the FOC approximation, as a function of the interatomic distance. Note that a logarithmic scale is used on both axes. Upper graph: before applying the laser: only ground state pairs exist, $\phi_e(r)=0$; the wave function $\phi_g(r)$ corresponds to a zero-energy scattering state: it oscillates in the short distance region, where the potential $U_g(r)$ is not negligible; for distances $r>1000a_0$, the amplitude is equal to the initial condensate density ρ_0. Lower graph: after applying a cw laser of intensity $I=10$ kW/cm^2 during 40 μs, a level of the excited potential has been populated: $\phi_e(r)$ oscillates up to the classical turning point of this level; the population transfer to this excited state is visible in the decrease of both the short-range amplitude of $\phi_g(r)$, and its very long-range amplitude corresponding to the condensate density. Note that a strong maximum emerges around $r\sim 55a_0$; it is the near-resonance signature of a weakly bound state in the ground-state channel. At large distances, $\phi_g(r)$ shows oscillations, interpreted as outward motion of "hot" correlated pairs ($T\sim 4$ to 40 μK).

we shall use the more general equations and numerical procedures described in this paper to investigate these situations.

VII. CONCLUSION

We have compared two many-body approximations for the time-dependent description of photoassociation and optically-induced Feshbach resonances in an atomic condensate: the first-order cumulant approximation and the reduced pair wave approximation. These approximations differ only in the way the influence of the mean field on a pair of condensate atoms is treated at short separations. Each approximation leads to a set of coupled equations describing the microscopic and macroscopic dynamics for a two-channel problem. We demonstrated that these equations can be solved numerically with realistic molecular potentials, which should prove essential when addressing experiments with chirped laser pulses, for which details of the interaction potentials may influence the dynamics.

From the general equations, we identified several regimes. We define the adiabatic regime when the excited molecular

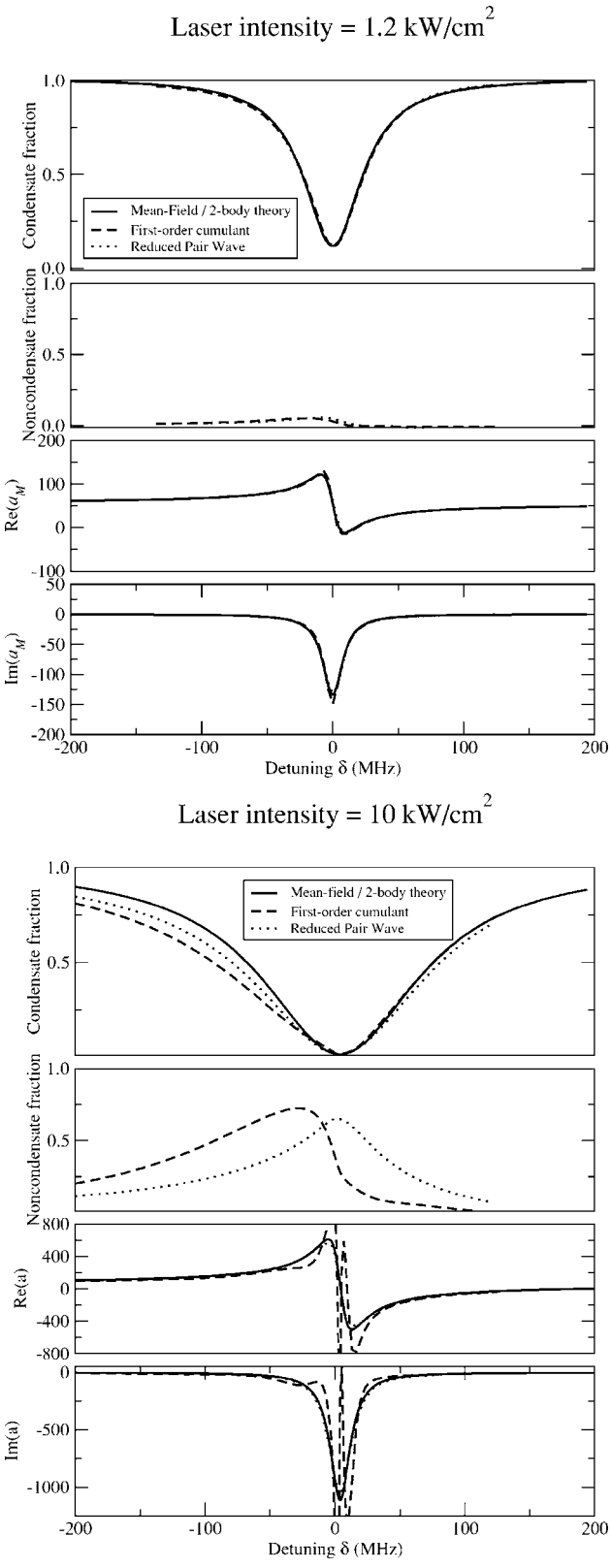

FIG. 8. Photoassociation line shape and optical Feshbach resonance: condensate, noncondensate fractions, and mean-field scattering length after 40 μs, as a function of the laser detuning δ from the bare molecular state (see Fig. 1). At high intensity (10 kW/cm^2), the first-order cumulant equations predict highly asymmetric behaviours with respect to the resonance.

channel is just an intermediate state during the collision of two condensate atoms. In contrast, we define the coherent regime when the excited channel gives rise to a molecular condensate having the features of a one-body condensate. In each of these two regimes, a mean-field theory is obtained when the pair correlation in the ground channel can be eliminated adiabatically. In the coherent regime, this leads to two coupled Gross-Pitaevskiĭ equations [25]. In the adiabatic regime, this leads to a single Gross-Pitaevskiĭ equation with a complex scattering length predicted by two-body theories. This is the usual regime investigated so far experimentally [20,41,57].

The condition for the breakdown of the mean-field approximation (or so-called rogue dissociation [56]) is different in each regime. We showed that, contrary to previous estimates [41,56], the condition for current experiments are under the adiabatic regime.

Solving the general equations numerically, we investigated the case of a sodium condensate where a photoassociation cw laser is turned on in conditions similar to the experiment of McKenzie *et al.* [41]. At high intensities ($\sim 10\ \mathrm{kW/cm^2}$), which could not be attained in [41] and where rogue dissociation is expected to occur, we observed the following effects:

(1) Ground-state correlated pairs of free atoms are produced. This agrees with the saturation predicted by Gasenzer [53]. The creation of such atom pairs can indeed strongly limit the final yield of ground-state molecules formed by spontaneous decay. However, Ref. [53] considered only a rapid turn on of the laser. By introducing a slower switching procedure, leading to a more adiabatic behaviour, the present work shows that the production of hot atom pairs may be decreased.

(2) The photoassociation rate of the condensate at short times is smaller than the rate predicted in the mean-field approximation. This limitation happens at much lower intensities than the unitary limit of the two-body theory. This effect has already been predicted by Javanainen and Mackie [56] in the coherent regime. We interpret it as the appearance of a dynamic many-body correlation in the condensate.

(3) The photoassociation line shape becomes asymmetric in the first-order cumulant approximation, while it remains symmetric in the reduced pair wave approximation.

We think this last point should be a good qualitative effect to experimentally distinguish between the two approximations. Future work will investigate the time dependence of the formation of stable molecules, via two-color or one-color experiments with pulsed lasers, using the theoretical and numerical tools developed in the present paper.

ACKNOWLEDGMENTS

P.N. is very grateful to Eite Tiesinga for his essential remarks on this work. Discussions with Arkady Shanenko, Paul Julienne, Thorsten Köhler, Christiane Koch, Eliane Luc-Koenig, and Philippe Pellegrini are gratefully acknowledged as well. This work was performed in the framework of the European Research Training Network "Cold Molecules," funded by the European Commission under Contract No. HPRN CT 2002 00290. P.N. acknowledges an invitation in Clarendon Laboratory, Oxford.

APPENDIX: IN-MEDIUM EFFECTIVE WAVE FUNCTIONS

1. General expressions

The in-medium pair wave function approach, as we may call it, was initiated by a series of papers by Cherny and Shanenko. Its aim is to have a many-body description of the dilute Bose gas which remains valid at short interatomic distances, so that interaction potentials with strong repulsive cores can be treated directly. The authors have mainly addressed the problem of the ground state for a homogeneous system. In Ref. [38], we have generalized some of their ideas to the inhomogeneous time-dependent case. We will recall here the derivation of the in-medium pair wave functions given in [38], limiting our discussion to the single channel case, and will show in addition how three-body wave functions can be constructed out of these pair wave functions. This will give a framework to interpret the first-order cumulant and reduced pair wave approximations used in this paper.

The starting point is to consider the reduced density matrices of the many-boson system. As these matrices are Hermitian, they can be diagonalized in a basis of orthogonal eigenvectors, associated with positive eigenvalues. For example, the following one-body, and two-body reduced density matrices can be diagonalized as follows:

$$\langle \hat{\psi}^\dagger(\mathbf{x})\hat{\psi}(\mathbf{y})\rangle = \sum_i \Psi_i^*(\mathbf{x})\Psi_i(\mathbf{y}), \tag{A1}$$

$$\tfrac{1}{2}\langle \hat{\psi}^\dagger(\mathbf{w})\hat{\psi}^\dagger(\mathbf{z})\hat{\psi}(\mathbf{x})\hat{\psi}(\mathbf{y})\rangle = \sum_i \Phi_i^*(\mathbf{w},\mathbf{z})\Phi_i(\mathbf{x},\mathbf{y}), \tag{A2}$$

where the Ψ_i are the eigenvectors of the one-body density matrix, and Φ_i are the eigenvectors of the two-body density matrix. We have normalized these vectors to their respective eigenvalues, which means that $N_i = \int d^3\mathbf{x}|\Psi_i(\mathbf{x})|^2$ is the eigenvalue associated with Ψ_i, and $M_i = \int d^3\mathbf{y}d^3\mathbf{x}|\Phi_i(\mathbf{x},\mathbf{y})|^2$ is the eigenvalue associated with Φ_i. As these eigenvectors have the form of wave functions, we call them effective one-body wave functions and effective pair wave functions. N_i is interpreted as the average number of particles of the system in the one-body state $|\Psi_i\rangle$, and M_i is interpreted as the average number of pairs in the two-body state $|\Phi_i\rangle$. We can check that $\Sigma_i N_i = N$ and $\Sigma_i M_i = \frac{1}{2}N(N-1)$, where N is the total number of particles in the system.

In the case of a condensate, a certain one-body wave function Ψ_0 has a macroscopic occupation number $N_0 \gg \Sigma_{i\neq 0} N_i$. In the U(1) symmetry breaking picture [46], this one-body wave function is identified with the condensate wave function, or order parameter $\langle\hat{\psi}\rangle$. According to the Bogoliubov prescription, the field operator $\hat{\psi}$ can then be decomposed into its average value Ψ_0 and a remaining fluctuating operator $\hat{\theta}$. Expanding the two-body density matrix (A2) with the Bogoliubov prescription, and refactorizing the expression, we showed that it can be written

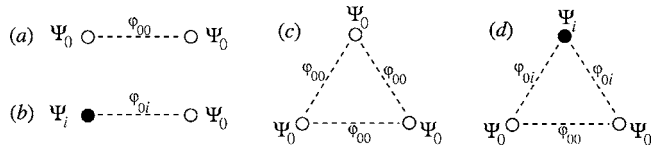

FIG. 9. Schematic representations of some effective in-medium wave functions in a condensate: the condensate pair wave function (*a*), the condensate-noncondensate pair wave function (*b*), the condensate three-body wave function (*c*), and the condensate-condensate-noncondensate three-body wave function (*d*). The circles indicate the asymptotic one-body behaviors, and the dashed lines represent the correlation.

$$\sum_{i=0}^{\infty} \Phi_{0i}^{*}(\mathbf{w},\mathbf{z})\Phi_{0i}(\mathbf{x},\mathbf{y}) + \tfrac{1}{2}\langle \hat{\theta}^{\dagger}(\mathbf{w})\hat{\theta}^{\dagger}(\mathbf{z})\hat{\theta}(\mathbf{x})\hat{\theta}(\mathbf{y})\rangle - \sum_{i=0}^{\infty} \Phi_{0i}'^{*}(\mathbf{w},\mathbf{z})\Phi_{0i}'(\mathbf{x},\mathbf{y}), \tag{A3}$$

where

$$\Phi_{00}(\mathbf{x},\mathbf{y}) = \frac{1}{\sqrt{2}}\Psi_0(\mathbf{x})\Psi_0(\mathbf{y}) + \Phi_{00}'(\mathbf{x},\mathbf{y}), \tag{A4}$$

$$\Phi_{0i}(\mathbf{x},\mathbf{y}) = \frac{\Psi_0(\mathbf{x})\Psi_i(\mathbf{y}) + \Psi_0(\mathbf{y})\Psi_i(\mathbf{x})}{\sqrt{2}} + \Phi_{0i}'(\mathbf{x},\mathbf{y}), \tag{A5}$$

for $i \neq 0$ and

$$\Phi_{00}'(\mathbf{x},\mathbf{y}) = \frac{1}{\sqrt{2}}\langle \hat{\theta}(\mathbf{x})\hat{\theta}(\mathbf{x})\rangle,$$

$$\Phi_{0i}'(\mathbf{x},\mathbf{y}) = \int d^3\mathbf{z}\frac{\Psi_i(\mathbf{z})}{\sqrt{2N_i}}\langle \hat{\theta}^{\dagger}(\mathbf{z})\hat{\theta}(\mathbf{x})\hat{\theta}(\mathbf{y})\rangle \quad \text{for } i \neq 0.$$

As the Φ_{0i}'s and Φ_{00} are orthogonal in the limit of large systems, we conclude that we have found the first pair wave functions of the diagonalized form (A2).

Φ_{00} is interpreted as the condensate-condensate wave function, i.e., the wave function for a pair of particles both coming from the condensed part (see Fig. 9 for a schematic representation). It is composed of two terms: an asymptotic term $\frac{1}{\sqrt{2}}\Psi_0(\mathbf{x})\Psi_0(\mathbf{y})$ corresponding to the free motion of two independent condensate particles, and a scattering term Φ_{00}' corresponding to their correlated motion due to their interaction. Similarly, Φ_{0i} for $i \neq 0$ is interpreted as the condensate-noncondensate wave function, i.e., the wave function for two particles, one coming from the condensed part and the other coming from the noncondensed part. It is also composed of an asymptotic term $\frac{\Psi_0(\mathbf{x})\Psi_i(\mathbf{y})+\Psi_0(\mathbf{y})\Psi_i(\mathbf{x})}{\sqrt{2}}$ (note the symmetrization) and a scattering term Φ_{0i}'. We can check that for a sufficiently large system the norm of Φ_{00} is $\frac{1}{2}N_0^2$, the number of condensate pairs, and the norm of Φ_{0i} is N_0N_i, the number of pairs involving a condensate particle and a noncondensate particle in state $|\Psi_i\rangle$. The presence of a condensate therefore implies a condensation of unbound pairs, as $\frac{1}{2}N_0^2 \gg \Sigma_{i\neq 0}N_0N_i$.

The last line of Eq. (A3) corresponds to the remaining pair wave functions of the system. We have no explicit expression for those, but if we assume that the noncondensate particles form an ideal gas (i.e., do not interact), we can use Wick's theorem to express the last line, and check that it is equal to

$$\sum_{0<i\leqslant j} \Phi_{ij}^{*}(\mathbf{w},\mathbf{z})\Phi_{ij}(\mathbf{x},\mathbf{y}),$$

with

$$\Phi_{ii}(\mathbf{x},\mathbf{y}) = \Psi_i(\mathbf{x})\Psi_i(\mathbf{y}),$$

$$\Phi_{ij}(\mathbf{x},\mathbf{y}) = \frac{\Psi_i(\mathbf{x})\Psi_j(\mathbf{y}) + \Psi_i(\mathbf{y})\Psi_j(\mathbf{x})}{\sqrt{2}} \quad \text{for } i \neq j,$$

which are indeed the expected pair wave functions for two noninteracting noncondensate atoms [63].

For convenience, we may rewrite the scattering terms appearing in (A4) and (A5) with multiplicative correlation functions φ_{0i} defined as follows:

$$\Phi_{00}(\mathbf{x},\mathbf{y}) \equiv \frac{1}{\sqrt{2}}\Psi_0(\mathbf{x})\Psi_0(\mathbf{y})\varphi_{00}(\mathbf{x},\mathbf{y}), \tag{A6}$$

$$\Phi_{0i}(\mathbf{x},\mathbf{y}) \equiv \frac{\Psi_0(\mathbf{x})\Psi_i(\mathbf{y}) + \Psi_0(\mathbf{y})\Psi_i(\mathbf{x})}{\sqrt{2}}\varphi_{0i}(\mathbf{x},\mathbf{y}). \tag{A7}$$

We call these functions φ_{0i} the reduced pair wave functions. Assuming that the particles must be decorrelated at large distances, we expect that the reduced pair wave functions tend to 1 at large distances. Thus, we may write $\varphi_{0i} = 1 + \varphi_{0i}'$ for convenience, with φ_{0i}' vanishing at large distances. Another important property is that for an interaction with a strong repulsive core, the probability of finding two particles close to each other should tend to zero at short distances; we therefore expect that the reduced pair wave functions φ_{0i} tend to zero at short distances. This property should ensure that they have a regularizing effect when multiplied with the interaction potential.

We can now write the equation of evolution for the condensate wave function

$$i\hbar\frac{\partial\Psi_0}{\partial t}(\mathbf{x},t) = H_{\mathbf{x}}\Psi_0(\mathbf{x},t) + \int d^3\mathbf{z}U(\mathbf{z}-\mathbf{x}) \times \langle \hat{\psi}^{\dagger}(\mathbf{z},t)\hat{\psi}(\mathbf{z},t)\hat{\psi}(\mathbf{x},t)\rangle, \tag{A8}$$

where $H_x = -\frac{\hbar^2\nabla^2}{2m} + V(\mathbf{x})$ is the one-body Hamiltonian for free atoms and U is the interaction potential. By expanding the quantum average in Eq. (A8) with the Bogoliubov prescription and refactorizing the terms, we find

$$\langle \hat{\psi}^{\dagger}(\mathbf{z})\hat{\psi}(\mathbf{z})\hat{\psi}(\mathbf{x})\rangle = \sqrt{2}\sum_{i=0}^{\infty}\Psi_i^{*}(\mathbf{z})\Phi_{0i}(\mathbf{z},\mathbf{x}). \tag{A9}$$

This gives a clear interpretation of this term in Eq. (A8): the condensate particles can collide either with another con-

densate particle or with a noncondensate particle. Each type of collision gives rise to a term looking like a scattering amplitude, where the corresponding two-body wave function is involved.

Similarly, the equation of evolution for the condensate pair wave function is

$$i\hbar\frac{\partial\Phi_{00}}{\partial t}(\mathbf{x},\mathbf{y},t) = (H_{\mathbf{x}} + H_{\mathbf{y}} + U(|\mathbf{x}-\mathbf{y}|))\Phi_{00}(\mathbf{x},\mathbf{y},t) + \left\{\int d^3\mathbf{z}U(\mathbf{z}-\mathbf{y}) \times\langle\hat{\psi}^\dagger(\mathbf{z},t)\hat{\psi}(\mathbf{z},t)\hat{\psi}(\mathbf{x},t)\hat{\psi}(\mathbf{y},t)\rangle\right\} + \{\mathbf{x}\leftrightarrow\mathbf{y}\}. \tag{A10}$$

By expanding the quantum average in Eq. (A10) in terms of cumulants, and collecting the terms, we find

$$\langle\hat{\psi}^\dagger(\mathbf{z})\hat{\psi}(\mathbf{z})\hat{\psi}(\mathbf{x})\hat{\psi}(\mathbf{y})\rangle = \sqrt{3!}\sum_{i=0}^{\infty}\Psi_i^*(\mathbf{z})\Omega_{00i}(\mathbf{z},\mathbf{x},\mathbf{y}), \tag{A11}$$

with the three-body wave functions

$$\Omega_{000}(\mathbf{z},\mathbf{x},\mathbf{y}) \equiv \frac{1}{\sqrt{3!}}\Psi_0(\mathbf{z})\Psi_0(\mathbf{x})\Psi_0(\mathbf{y})[1+\varphi'_{00}(\mathbf{z},\mathbf{x}) + \varphi'_{00}(\mathbf{z},\mathbf{y}) + \varphi'_{00}(\mathbf{x},\mathbf{y})] + \Omega'_{000}(\mathbf{z},\mathbf{x},\mathbf{y}),$$

$$\begin{aligned}\Omega_{00i}(\mathbf{z},\mathbf{x},\mathbf{y}) \equiv \frac{1}{\sqrt{3!}}\{&\Psi_i(\mathbf{z})\Psi_0(\mathbf{x})\Psi_0(\mathbf{y})[1+\varphi'_{0i}(\mathbf{z},\mathbf{x})+\varphi'_{0i}(\mathbf{z},\mathbf{y}) + \varphi'_{00}(\mathbf{x},\mathbf{y})] + \Psi_i(\mathbf{y})\Psi_0(\mathbf{z})\Psi_0(\mathbf{x})[1+\varphi'_{00}(\mathbf{z},\mathbf{x}) \\ &+ \varphi'_{0i}(\mathbf{z},\mathbf{y})+\varphi'_{0i}(\mathbf{x},\mathbf{y})] + \Psi_i(\mathbf{x})\Psi_0(\mathbf{z})\Psi_0(\mathbf{y}) \\ &\times[1+\varphi'_{0i}(\mathbf{z},\mathbf{x})+\varphi'_{00}(\mathbf{z},\mathbf{y})+\varphi'_{0i}(\mathbf{x},\mathbf{y})]\} \\ &+ \Omega'_{00i}(\mathbf{z},\mathbf{x},\mathbf{y}),\end{aligned}$$

where

$$\Omega'_{000}(\mathbf{z},\mathbf{x},\mathbf{y}) = \frac{1}{\sqrt{3!}}\langle\hat{\theta}(\mathbf{z})\hat{\theta}(\mathbf{x})\hat{\theta}(\mathbf{y})\rangle^c,$$

$$\Omega'_{00i}(\mathbf{z},\mathbf{x},\mathbf{y}) = \int d^3\mathbf{w}\frac{\Psi_i(\mathbf{w})}{\sqrt{3!}N_i}\langle\hat{\theta}^\dagger(\mathbf{w})\hat{\theta}(\mathbf{z})\hat{\theta}(\mathbf{x})\hat{\theta}(\mathbf{y})\rangle^c,$$

and $\langle\cdots\rangle^c$ is the cumulant notation [34].

We note that the first term of each three-body wave functions is not the wave function of independent particles, contrary to what we found with pair wave functions. Indeed, it already contains some pair correlation through the terms φ'. However, these pair correlations are not complete. For an interaction with a strong repulsive core, the probability for finding three atoms very close to one another must tend to zero. But here, the first term of each three-body wave function does not vanish when $\mathbf{x}\approx\mathbf{y}\approx\mathbf{z}$. We think this is because this first term is only the asymptotic behavior of the three-body wave function at large distances. The terms Ω' must contain stronger correlations at short distances. We expect that at short distances, the three-body wave functions are in fact fully correlated through a product of reduced pair wave functions akin to a Jastrow wave function [51]

$$\Omega_{000}(\mathbf{z},\mathbf{x},\mathbf{y}) \equiv \frac{1}{\sqrt{3!}}\Psi_0(\mathbf{z})\Psi_0(\mathbf{x})\Psi_0(\mathbf{y})\varphi_{00}(\mathbf{z},\mathbf{x})\varphi_{00}(\mathbf{z},\mathbf{y}) \times\varphi_{00}(\mathbf{x},\mathbf{y}) + \Omega''_{000}(\mathbf{z},\mathbf{x},\mathbf{y}),$$

$$\begin{aligned}\Omega_{00i}(\mathbf{z},\mathbf{x},\mathbf{y}) \equiv \frac{1}{\sqrt{3!}}[&\Psi_i(\mathbf{z})\Psi_0(\mathbf{x})\Psi_0(\mathbf{y})\varphi_{0i}(\mathbf{z},\mathbf{x})\varphi_{0i}(\mathbf{z},\mathbf{y}) \times\varphi_{00}(\mathbf{x},\mathbf{y}) + \Psi_i(\mathbf{y})\Psi_0(\mathbf{z})\Psi_0(\mathbf{x})\varphi_{00}(\mathbf{z},\mathbf{x}) \\ &\times\varphi_{0i}(\mathbf{z},\mathbf{y})\varphi_{0i}(\mathbf{x},\mathbf{y}) + \Psi_i(\mathbf{x})\Psi_0(\mathbf{z})\Psi_0(\mathbf{y}) \\ &\times\varphi_{0i}(\mathbf{z},\mathbf{x})\varphi_{00}(\mathbf{z},\mathbf{y})\varphi_{0i}(\mathbf{x},\mathbf{y})] + \Omega''_{00i}(\mathbf{z},\mathbf{x},\mathbf{y}).\end{aligned}$$

This is the most natural structure which preserves the symmetry of the three-body wave functions and leads to a zero probability at short distances. The remaining terms Ω'' are supposed to contain the three-body correlations which cannot be expressed in terms of two-body correlations. Note again that the norm of Ω_{000} is $\frac{1}{3!}N_0^3$ corresponding to the number of condensate triplets, while the norm of Ω_{00i} is $\frac{1}{2}N_0^2N_i$, corresponding to the number of triplets involving two condensate particles and one particle in the noncondensate state $|\Psi_i\rangle$.

The interpretation of (A11) appearing in Eq. (A10) is again very simple: the pairs of condensate atoms can collide either with another condensate atom, or with a noncondensate atom. Each type of collision is accounted for by a scattering amplitudelike term, involving the corresponding three-body wave function.

2. Simplified expressions

Neglecting the collisions with noncondensate particles as well as the three-body correlation Ω''_{000}, we can express the quantum averages in terms of only the condensate wave function $\Psi\equiv\Psi_0$ and the condensate pair wave function $\Phi=\sqrt{2}\Phi_{00}$

$$\langle\hat{\psi}^\dagger(\mathbf{w})\hat{\psi}(\mathbf{z})\hat{\psi}(\mathbf{x})\rangle \approx \Psi^*(\mathbf{w})\Phi(\mathbf{z},\mathbf{x}), \tag{A12}$$

$$\langle\hat{\psi}^\dagger(\mathbf{w})\hat{\psi}^\dagger(\mathbf{z})\hat{\psi}(\mathbf{x})\hat{\psi}(\mathbf{y})\rangle \approx \Phi^*(\mathbf{w},\mathbf{z})\Phi(\mathbf{x},\mathbf{y}), \tag{A13}$$

$$\langle\hat{\psi}^\dagger(\mathbf{w})\hat{\psi}(\mathbf{z})\hat{\psi}(\mathbf{x})\hat{\psi}(\mathbf{y})\rangle \approx \Psi^*(\mathbf{w})\frac{\Phi(\mathbf{z},\mathbf{x})\Phi(\mathbf{z},\mathbf{y})\Phi(\mathbf{x},\mathbf{y})}{\Psi(\mathbf{x})\Psi(\mathbf{y})\Psi(\mathbf{z})}. \tag{A14}$$

Note that all these expressions respect the symmetry of the quantum averages by exchange of coordinates. Both the first-order cumulant and reduced pair wave approximation used in this paper imply the relations (A12) and (A13). However, they differ on the expression of the average (A14) which determines the mean-field potential experienced by a pair of condensate atoms.

a. Reduced pair wave approximation

The reduced pair wave approximation (assumption *H*2 in our previous work [38]) is equivalent to

$$\langle \hat{\psi}^\dagger(\mathbf{w})\hat{\psi}(\mathbf{z})\hat{\psi}(\mathbf{x})\hat{\psi}(\mathbf{y})\rangle \approx \Psi^*(\mathbf{w})\frac{\Phi(\mathbf{z},\mathbf{x})\Phi(\mathbf{x},\mathbf{y})}{\Psi(\mathbf{x})},$$

in other words, we neglect the correlation between **z** and **y** in (A14). As a result, the reduced pair wave function φ_{00} obeys exactly the two-body Schrödinger equation in free space. Note that this assumption breaks the symmetry of the quantum average (A14). It leads to Eqs. (14) and (15) in this paper.

b. First-order cumulant approximation

The first-order cumulant approximation [34] is equivalent to

$$\langle \hat{\psi}^\dagger(\mathbf{w})\hat{\psi}(\mathbf{z})\hat{\psi}(\mathbf{x})\hat{\psi}(\mathbf{y})\rangle \approx \Psi^*(\mathbf{w})\Phi(\mathbf{z},\mathbf{x})\Psi(\mathbf{y}),$$

in other words, we neglect the correlation between **z** and **y**, and **x** and **y** in (A14). Note that this assumption breaks the symmetry of the quantum average (A14). It leads to Eqs. (8) and (9) in this paper. One can see that the reduced pair wave approximation brings a partial correction to the first-order cumulant approximation, by taking into account an extra correlation.

[1] B. E. Sauer, J. Wang, and E. A. Hinds, Bull. Am. Phys. Soc. **39**, 1060 (1994).
[2] E. A. Hinds, Phys. Scr. **T70**, 34 (1997).
[3] D. J. Heinzen, R. Wynar, P. D. Drummond, and K. V. Kheruntsyan, Phys. Rev. Lett. **84**, 5029 (2000).
[4] E. A. Donley, N. R. Claussen, S. T. Thompson, and C. E. Wieman, Nature (London) **417**, 529 (2002).
[5] N. R. Claussen, E. A. Donley, S. T. Thompson, and C. E. Wieman, Phys. Rev. Lett. **89**, 010401 (2002).
[6] J. Herbig, T. Kraemer, M. Mark, T. Weber, C. Chin, H.-C. Nägerl, and R. Grimm, Science **301**, 1510 (2003).
[7] K. Xu, T. Mukaiyama, J. R. Abo-Shaeer, J. K. Chin, D. E. Miller, and W. Ketterle, Phys. Rev. Lett. **91**, 210402 (2003).
[8] S. Dürr, T. Volz, A. Marte, and G. Rempe, Phys. Rev. Lett. **92**, 020406 (2004).
[9] C. A. Regal, C. Ticknor, J. L. Bohn, and D. S. Jin, Nature (London) **424**, 47 (2003).
[10] M. W. Zwierlein, C. A. Stan, C. H. Schunck, S. M. F. Raupach, S. Gupta, Z. Hadzibabic, and W. Ketterle, Phys. Rev. Lett. **91**, 250401 (2003).
[11] K. E. Strecker, G. B. Partridge, and R. G. Hulet, Phys. Rev. Lett. **91**, 080406 (2003).
[12] J. Cubizolles, T. Bourdel, S. J. J. M. F. Kokkelmans, G. Shlyapnikov, and C. Salomon, Phys. Rev. Lett. **91**, 240401 (2003).
[13] S. Jochim, M. Bartenstein, A. Altmeyer, G. Hendl, C. Chin, J. H. Denschlag, and R. Grimm, Phys. Rev. Lett. **91**, 240402 (2003a).
[14] S. Jochim, M. Bartenstein, A. Altmeyer, G. Hendl, S. Riedl, C. Chin, J. H. Denschlag, and R. Grimm, Science **302**, 2101 (2003).
[15] C. A. Regal, M. Greiner, and D. S. Jin, Phys. Rev. Lett. **92**, 040403 (2004).
[16] P. O. Fedichev, Y. Kagan, G. V. Shlyapnikov, and J. T. M. Walraven, Phys. Rev. Lett. **77**, 2913 (1996).
[17] J. L. Bohn and P. S. Julienne, Phys. Rev. A **56**, 1486 (1997).
[18] V. Kokoouline, J. Vala, and R. Kosloff, J. Chem. Phys. **114**, 3046 (2001).
[19] F. K. Fatemi, K. M. Jones, and P. D. Lett, Phys. Rev. Lett. **85**, 4462 (2000).
[20] M. Theis, G. Thalhammer, K. Winkler, M. Hellwig, G. Ruff, R. Grimm, and J. H. Denschlag, Phys. Rev. Lett. **93**, 123001 (2004).
[21] G. Thalhammer, M. Theis, K. Winkler, R. Grimm, and J. H. Denschlag, Phys. Rev. A **71**, 033403 (2005).
[22] C. P. Koch, F. Masnou-Seeuws, and R. Kosloff, Phys. Rev. Lett. **94**, 193001 (2005).
[23] C. P. Koch, J. P. Palao, R. Kosloff, and F. Masnou-Seeuws, Phys. Rev. A **70**, 013402 (2004).
[24] P. D. Drummond, K. V. Kheruntsyan, and H. He, Phys. Rev. Lett. **81**, 3055 (1998).
[25] E. Timmermans, P. Tommasini, M. Hussein, and A. Kerman, Phys. Rep. **315**, 199 (1999).
[26] A. Vardi, V. A. Yurovksi, and J. R. Anglin, Phys. Rev. A **64**, 063611 (2001).
[27] S. J. J. M. F. Kokkelmans and M. J. Holland, Phys. Rev. Lett. **89**, 180401 (2002).
[28] M. Mackie, K.-A. Suominen, and J. Javanainen, Phys. Rev. Lett. **89**, 180403 (2002).
[29] T. Köhler, T. Gasenzer, P. S. Julienne, and K. Burnett, Phys. Rev. Lett. **91**, 230401 (2003).
[30] P. D. Drummond and K. V. Kheruntsyan, Phys. Rev. A **70**, 033609 (2004).
[31] J. Vala, O. Dulieu, F. Masnou-Seeuws, P. Pillet, and R. Kosloff, Phys. Rev. A **63**, 013412 (2000).
[32] E. Luc-Koenig, R. Kosloff, F. Masnou-Seeuws, and M. Vatasescu, Phys. Rev. A **70**, 033414 (2004).
[33] E. Luc-Koenig, M. Vatasescu, and F. Masnou-Seeuws, Eur. Phys. J. D **31**, 239 (2004).
[34] T. Köhler and K. Burnett, Phys. Rev. A **65**, 033601 (2002).
[35] T. Köhler, T. Gasenzer, and K. Burnett, Phys. Rev. A **67**, 013601 (2003).
[36] K. Góral, T. Köhler, T. Gasenzer, and K. Burnett, J. Mod. Opt. **51**, 1731 (2004).
[37] J. Fricke, Ann. Phys. (Paris) **252**, 479 (1996).
[38] P. Naidon and F. Masnou-Seeuws, Phys. Rev. A **68**, 033612 (2003).
[39] A. Y. Cherny and A. A. Shanenko, Phys. Rev. E **62**, 1646 (2000).
[40] A. Y. Cherny and A. A. Shanenko, Phys. Lett. A **293**, 287 (2002).
[41] C. McKenzie, J. H. Denschlag, H. Häffner, A. Browaeys, L. E. de Araujo, F. Fatemi, K. M. Jones, J. Simsaran, D. Cho, A. Simoni *et al.*, Phys. Rev. Lett. **88**, 120403 (2002).

[42] J. L. Bohn and P. S. Julienne, Phys. Rev. A **60**, 414 (1999).
[43] F. Masnou-Seeuws and P. Pillet, Adv. At., Mol., Opt. Phys. **47**, 53 (2001).
[44] L. Allen and J. Eberly, *Optical Resonance and Two-Level Atoms* (Dover, New York, 1987).
[45] L. Pitaevskiĭ and S. Stringari, *Bose-Einstein Condensation* (Oxford University Press, 2003).
[46] A. J. Leggett, Rev. Mod. Phys. **73**, 307 (2001).
[47] E. Fermi, Ric. Sci. **7**, 13 (1936).
[48] K. Huang, *Statistical Mechanics* (Wiley, New York, 1987).
[49] T. D. Lee, K. Huang, and C. N. Yang, Phys. Rev. **106**, 1135 (1957).
[50] S. J. J. M. F. Kokkelmans, J. N. Milstein, M. L. Chiofalo, R. Walser, and M. J. Holland, Phys. Rev. A **65**, 053617 (2002).
[51] R. Jastrow, Phys. Rev. **98**, 1479 (1955).
[52] V. I. Yukalov, Phys. Rev. A **42**, 3324 (1990).
[53] T. Gasenzer, Phys. Rev. A **70**, 021603(R) (2004).
[54] A. Y. Cherny and J. Brand, Phys. Rev. A **70**, 043622 (2004).
[55] A. Fioretti, D. Comparat, A. Crubellier, O. Dulieu, F. Masnou-Seeuws, and P. Pillet, Phys. Rev. Lett. **80**, 4402 (1998).
[56] J. Javanainen and M. Mackie, Phys. Rev. Lett. **88**, 090403 (2002).
[57] K. Winkler, G. Thalhammer, M. Theis, H. Ritsch, R. Grimm, and J. H. Denschlag, Phys. Rev. Lett. **95**, 063202 (2005).
[58] V. Kokoouline, O. Dulieu, R. Kosloff, and F. Masnou-Seeuws, J. Chem. Phys. **110**, 9865 (1999).
[59] W. H. Press, S. A. Teukolsky, W. T. Vettering, and B. P. Flannery, *Numerical Recipes* (2nd edition) (Cambride University Press, Cambridge, 1996), www.nr.com.
[60] P. Pellegrini, Ph.D. thesis (2003).
[61] M. Marinescu and A. Dalgarno, Phys. Rev. A **52**, 311 (1995).
[62] To be complete, one should also include the bound states of the potential. This has no major consequence on the following analysis.
[63] However, Wick's theorem, like the Hartree-Fock decoupling, induces a double counting of noncondensate particles in the same state which we have missed in Ref. [38]. Equation (A23) of this reference should not contain the factor $\sqrt{2}$. Note however that this is an artifact of the Wick/Hartree-Fock decoupling and that the factor $\sqrt{2}$ is really present for a noninteracting system, as can be checked by direct calculation.